Detailed Experimental Set Up

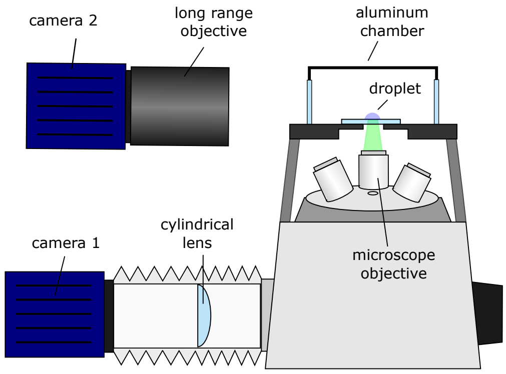

Figure 1: A detailed sketch of the experimental set up.

As depicted in the figure above, experiments are performed with sessile evaporating water droplets in an aluminium chamber at room conditions, with humidity between 40 %-45 % and 20 ℃ temperature. The chamber is not pressurized but partly open to the atmosphere. A droplet is gently deposited on a glass slide, which is at the same time held by a thick aluminum holder (at room temperature) that serves also as heat sink. The chamber, which is also in contact with the holder, protects the droplet from air currents that strongly disturb the droplet's surface flow. The temperature at the aluminium chamber and holder is recorded during the evaporation process to make sure that there are no external temperature variations. There is not additional control of the temperature in the system. The droplet contains a very low concentration of fluorescent polymeric particles (below 0.001 % w/w). They are visualized through the glass slide using an epifluorescence inverted microscope Zeiss Axiovert in combination with a high-sensitivity sCMOS camera (camera 1). A wide range of recording speeds from 0.01 fps up to 100 fps can be chosen. The experiments shown were recorded at 1 fps, which was enough to capture the particle motion at good temporal and spatial resolution. Simultaneously, a side view of the droplet is obtained through a glass window of the chamber in order to measure the droplet profile in time and therefore obtain the contact angle evolution in time and the evaporation rate (camera 2). Data regarding the evaporation rates obtained in the different experiments is shown below. Illumination is provided either by a pulsed diode-pumped laser or by a low-power continuous laser with 532 nm wavelength. This configuration provided a maximum measurement volume of about $1500 \times 1500 \times 300$ μm^3 with an estimated uncertainty in the particle position determination of ± 1 μm in the z-direction and less than ± 0.1 μm in the x- and y-direction. The optical arrangement consisted of EC Plan-Neofluar 10x/0.3 microscope objective lens and a cylindrical lens with focal length $f_{\mathrm{cyl}} = 300$ mm placed in front of the CCD sensor of the camera. The cylindrical lens is typically used in astigmatism particle tracking velocimetry (APTV) to introduce a controlled aberration in the particle shape. Consequently, an image of a spherical particle obtained in such a system shows a characteristic elliptical shape unequivocally related to its depth-position z.

APTV working principle

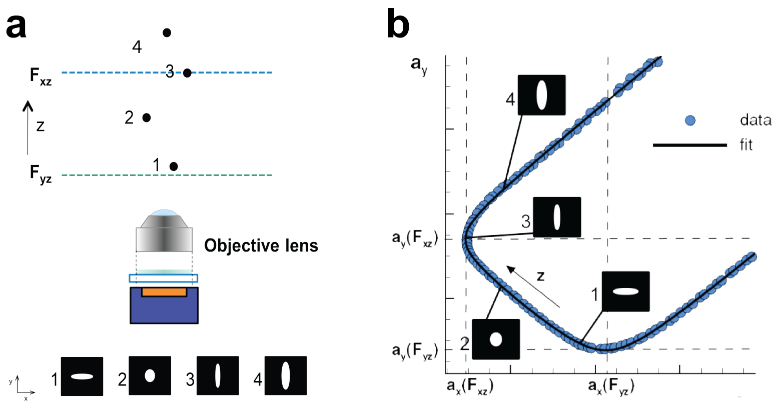

Figure 2: The APTV working principle: (a) The particle image on the camera will change depending on the particle distance to the main focal planes of the astigmatic optical system, Fxz and Fyz. (b) The principal diameters in the x- and y-direction of the elliptical particle images collapse to a parametric curve, where the parameter is the depth position z. A reference curve obtained through a calibration procedure is used to calculate the z-position from the measured particle image diameters

Figure 2 shows the working principle of APTV: Due to the astigmatic optics, a single focal plane is not present any longer. Two principal focal planes, Fxz and Fyz, can be identified, corresponding to the x- and y-direction in the image plane, respectively. Particle 1 is closer to Fyz so that its image will result in-focus (smaller) in the y-direction and out-of-focus (larger) in the x-direction. The opposite happens for particle 3. In general, the particle images assume a characteristic elliptical shape directly related with their z-position. If one measures the principal diameters (x- and y-direction) of the particle images across all the measurement volume they will collapse on a typical calibration curved as depicted in Figure 2. A calibration procedure is performed to obtain a reference calibration curve and used afterward to obtain the z-position of the measured particles. The x- and y-position is obtained in a straightforward fashion from the centroid of the particle images. More information can be found in the literature: Cierpka, Rossi, Segura & Kähler. *Measurement Science and Technology*, 22:015401, (2011); Rossi & Kähler. *Experiments in Fluids*, 55(9) 1809-1813, (2014); Barnkob, Kähler & Rossi. *Lab on a Chip*, 15:3556-3560 (2015).

Evaporation Rates

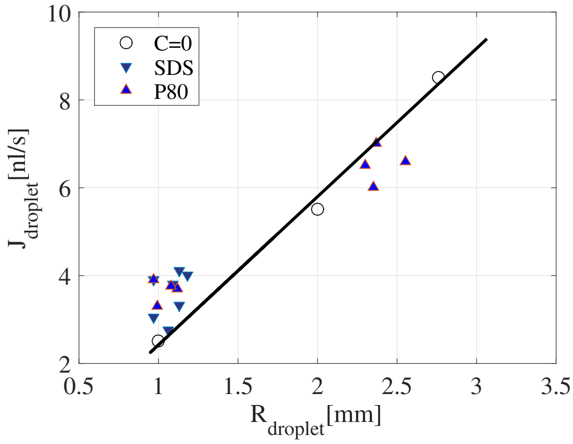

Figure 3: Evaporation rate of droplets with different radii at 20℃ room temperature (as measured on the aluminium holder working as heat sink), and humidities ranging from 40% to 45%.

Figure 3 shows the evaporation rate of droplets with different radii at 20℃ room temperature (as measured on the aluminium holder working as heat sink), and humidities ranging from 40% to 45%. Three different test cases without any surfactant were tested at different radii to check the linear dependence of the evaporation rate with the droplet radius. The data shown in the paper corresponds to droplets with radii in the range of 1 mm to 2.5 mm. The spreading of the data does not follow any clear correlation with the amount or the type of surfactant employed, and can be due to small humidity variations among the different experiments.

Video Captions

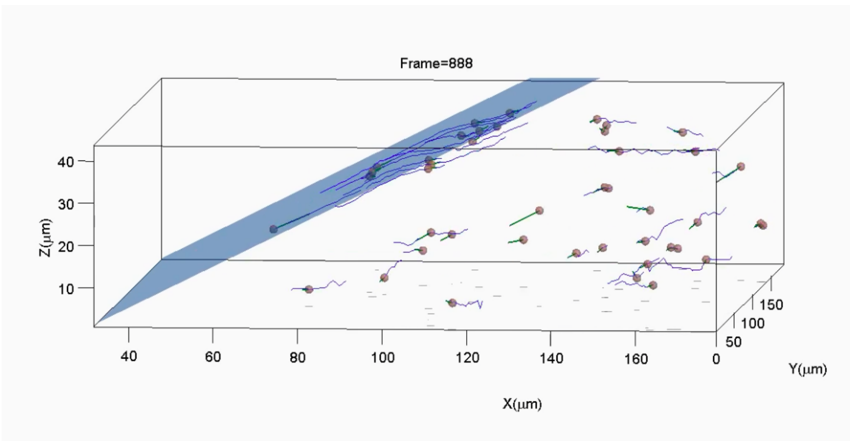

- **Video1-water.mp4:** Surfactant-free evaporating droplet of water with particle tracers

  This video shows experimental data of a water evaporating droplet of 5 mm diameter, but focusing in the area close to the contact line (at the left side), the water surface is represented by a bluish plane. The total observed volume in this case is circa 150 × 150 × 50 μm^3. In all the following videos the droplet surface (here in blue) is reconstructed from the measured contact angle in time and the droplet radius.

- **Video2-water-velo-CA.m4v** Surfactant-free evaporating droplet of water with particle flow tracers

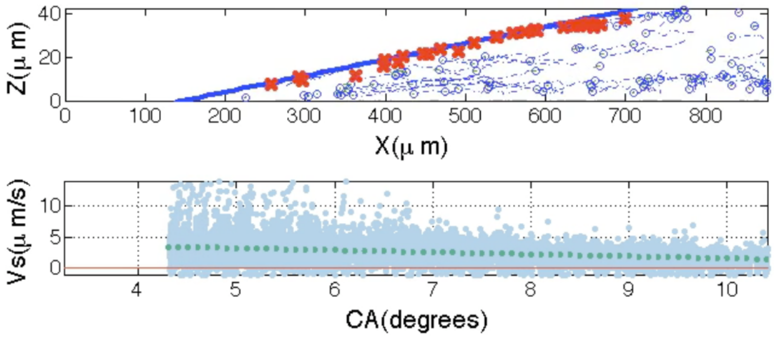

This video shows experimental data of a water evaporating droplet of 5 mm diameter. Unlike the previous one, this one covers a larger area, circa $800 \times 500\ \mu m^2$. In the bottom subfigure the surface velocity values $V_s(\mu m/s)$ of those particles close enough to the surface are plotted vs. the droplet's contact angle. Particles at a distance to the surface below 5 μm are shown as red crosses and its velocity measured. The green dark dotted line of points represents the average velocity detected. This strategy yields pretty noisy data since the instantaneous particle velocity is highly affected by the particle's Brownian motion. The trend is nonetheless clear and particle velocity increases slowly as time evolves (and contact angle decreases), contrary to what has been often reported in the literature. Note that the velocity data shown in Figure 3 in the main text have been obtained by fitting velocity profiles of particles within a certain radial position and time interval which was slightly adjusted for every experiment. This approach reduced the thermal noise and gave more reproducible and clear results.

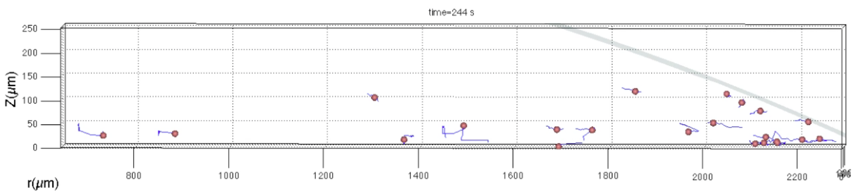

- **Video3-P80-1CMC.mp4** Evaporating water droplet containing P80 at its CMC with particle flow tracers

  The video shows a water droplet of 4 mm containing Polysorbate 80 at its critical micellar concentration. Notice the lack of dynamics in contrast with the previous videos of surfactant-free droplets. Also worth mentioning that only particles that travel a significant distance are plotted.

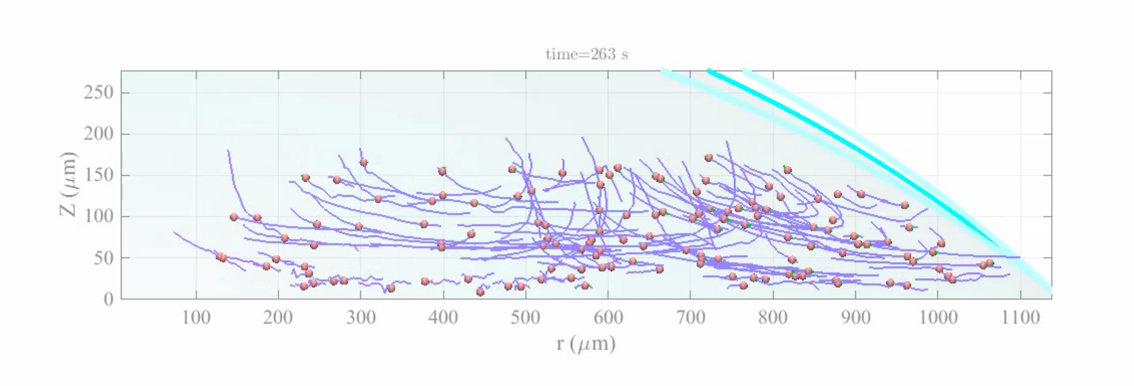

- **Video4-SDS-50CMC.mp4** Evaporating water droplet containing SDS at 50 × CMC with particle flow tracers

  The video shows a water droplet of 2 mm diameter containing sodium dodecyl sulfate (SDS) at 50 times its critical micellar concentration. Due to their reduced size, such droplets do not show such strong dynamics when they are surfactant-free. However, when SDS was added above its CMC, the dynamics become even stronger than thermal-driven Marangoni flows that develop spontaneously in such systems.